Benign and Malignant Pattern Identification in Cytopathological Images of Thyroid Nodules using Gabor Filter and Neural Networks

(Pattern Identification in Cytopathological Images)

B.Gopinath[1] and R.Santhi[2]
[1]*Department of Electronics and Communication Engineering, Madanapalle Institute of Technology & Science, Madanapalle, Andhra Pradesh, India*
gopiphd@yahoo.com

[2]*Department of Biochemistry, PSG College of Arts & Science, Coimbatore, Tamilnadu, India*
santhiakash@yahoo.com

***Abstract*— This research work presents an automated pattern recognition system to discriminate benign and malignant thyroid nodules using Gabor features based Neural Network classifiers. In the preprocessing step, the required regions of multi-stained Fine Needle Aspiration Cytology images of thyroid nodules are automatically cropped. Then, the segmentation of foreground information is performed using mathematical morphology technique. In the post processing step, the significant statistical features are extracted from the segmented images with the help of Gabor filter under various frequencies and orientations. Finally, the benign and malignant image patterns are discriminated using Elman Neural Network and Auto-associative Neural Network. Based on the performance analysis, the discrimination accuracy of 93.33% is obtained by the Elman Neural Network classifier for the statistical features extracted by Gabor filter bank. However, the auto-associative Neural Network classifier reports a highest discrimination accuracy of 96.66% for the same configuration. This automated discrimination system can be used as a second opinion tool for thyroid nodule analysis by the pathologists.**

***Keywords*—Cytology; Fine Needle Aspiration; Gabor Filter; Morphology; Neural Network; Segmentation**

I. INTRODUCTION

The thyroid is a small gland located in the lower part of the human neck which is responsible for producing thyroid hormones. These thyroid hormones deliver energy to cells of the human body and control metabolism [1]. The unwanted abnormal growth of cells around thyroid gland in the neck can form a mass of tissue that is called as thyroid nodules. Most of these thyroid nodules are not cancerous (benign). However, about 5-10% of thyroid nodules are discovered as cancerous (malignant). The medical research community is working on the strong identification of benign and malignant thyroid nodules so that unnecessary and costly invasive procedures can be avoided for patients with benign nodules.

The Fine Needle Aspiration Cytology (FNAC) is the most common procedure to determine benign and malignant types of cells present in the thyroid nodules. In FNAC procedure, a small needle is inserted into the thyroid nodule to collect the biopsy sample material. The smears are, then, prepared on glass slides using the sample material and screened by a pathologist under a microscope. Under examination, a trained pathologist can assess the appropriate changes in the distribution of the cells across the sample and comes to a conclusion. The result of FNAC procedure depends on the experience of the pathologist who is performing the procedure and hence, this judgment may lead to considerable variation. Although the standard manual screening techniques are successful in discriminating benign and malignant states of thyroid nodules, they still have serious drawbacks among which misdiagnosis is the most significant.

To overcome these problems and improve the reliability of diagnosis, it is necessary to develop an efficient automated discrimination system for screening FNAC cytopathological images using image processing techniques. Furthermore, the automated diagnosis system can provide an advantage of processing huge amount of medical images in a short period of time.

Many research works are being carried out for developing automated discrimination of microscopic medical images. Karakitsos et al. [2] investigated the application of Learning Vector Quantization (LVQ) neural networks in discriminating benign and malignant thyroid nodules and achieved diagnosis accuracy of 97.8%, employing the specialized May-Grunwald-Giemsa staining protocol. A multimodal cell analysis approach was proposed for automatic segmentation and discrimination of cell nuclei in cytopathological microscopic images using Bayesian and k-NN classifiers. This study reported an optimal recognition accuracy of 86.1% for Bayesian classifier and 87.5% for k-NN classifier [3]. Lezoray et al. [4] proposed an automatic segmentation of the cellular objects with color watershed transform and classification of cells from Broncho Alveolar Lavage using k-means classifier. Shapiro et al. [5] studied the performance of artificial neural networks (NNs) for the diagnosis of thyroid follicular tumors using cytologic features, morphometric parameters and density features of chromatin texture. ANN distinguished an adenoma or a carcinoma in 87% of cases using density features of chromatin texture. However, NN produced the correct diagnosis in 93% of cases with cytologic features and 97% of cases with morphometric parameters. Wang et al. [6] developed an automatic scheme that identified chromosomes in metaphase stage and classified them into analyzable and un-analyzable groups to diagnose cancers and genetic diseases using decision tree (DT) and NN classifiers in optical microscopic images. Daskalakis et al. [7] carried out the discrimination of benign from malignant thyroid nodules using routinely H&E stained cytological images by developing a multi-classifier system. It classified thyroid nodules using H&E stained FNAB cytological images and classification accuracy of 89.6% and 95.7% were reported for probabilistic neural network (PNN) single classifier and fusion of classifiers respectively.

Gopinath et al. [8] conducted experiment with ENN classifier trained by Gabor filter based features which reported a highest discrimination accuracy of 93.33%. In the previous work, Gopinath et al. [9] experimentally tested decision tree, k-NN, ENN and SVM classifiers among which the ENN and SVM classifiers exhibited superior diagnostic accuracy of 90% to recognize benign and malignant thyroid nodules using the statistical textural features derived by two-level wavelet decomposition. The improved diagnostic accuracy of 96.66% achieved for the multiple classifiers with majority voting of k-NN, ENN and SVM classifiers and linear combination of single classifiers.

In the present work, testing and evaluation of auto-associative neural network is performed, as a classifier, along with Gobar filter bank features for the same configuration of image sets investigated in [7] and [8].

II. AUTO-CROPPING AND SEGMENTATION

The multi-stained thyroid cytopathological FNAC images, stained by various types of stains, are obtained from an on-line image atlas source of the Papanicolaou Society of Cytopathology, which are reviewed and approved by the atlas committee [10]. The training image set consists of 80 images among which 40 are benign and remaining 40 are malignant images, whereas the testing image set has 30 images among which 10 are benign and 20 are malignant images.

The discrimination ability of the system is generally affected by the background staining information and hence, the unwanted information is removed in the pre-processing step. The FNAC images are initially auto-cropped to obtain high density cell portion followed by thresholding operation. Subsequently, mathematical morphology image segmentation methodology is applied on multi-stained FNAB images to segment the required cell regions of thyroid nodules.

To implement auto-cropping technique, a 256*x*256 cropping window is generated and moved over the entire image and mean value is calculated for each window.

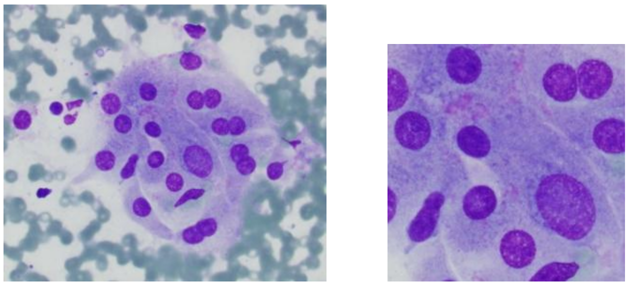

Fig. 1 Original and cropped images of FNAC thyroid images

Statistically, a window with high density cell region in the image will have least mean value. Thus, a window having least mean value is cropped and used for further processing which will improve the discrimination accuracy. The original image and cropped image are shown in Fig. 1.

Thresholding is the most common method of separating objects from its background in a given image. A global thresholding approach with a constant thresholding value is used in this work. An appropriate threshold value is automatically calculated using Otsu's method [11] to classify image pixels into one of two classes which means objects and background.

The basic region based mathematical morphology methodology is used in this work for extracting shape and size information from the given thyroid FNAC images. In general, the morphological operators transform the original image into another image by the interaction between the FNAC images and the structuring element of a certain shape and size. Geometric features of the FNAC images that are similar in shape and size to the structuring element are preserved, while other features are suppressed. The auto-cropped and thresholded FNAC images are treated with the morphological operators opening and closing along with structuring elements. If sets *I* and *Se* are referred to as the input image and structuring element, respectively, and *s* is an element of *Se*, then opening and closing are defined as,

$$Opening: (I \circ Se) = (I \ominus Se) \oplus Se \quad (1)$$

$$Closing: (I \bullet Se) = (I \oplus Se) \ominus Se \quad (2)$$

where,

$$Dilation: I \oplus Se = \bigcup_{s \in Se} I_s \qquad (3)$$

$$Erosion: I \ominus Se = \bigcap_{s \in Se} I_{-s} \qquad (4)$$

III. Gabor Filter and Feature Extraction

Texture features of an image can be used as powerful descriptors for the classification problem and they can be derived using statistical and structural methods. The statistical methods are motivated from Julesz's findings that human visual systems can easily recognize textured objects based on the statistical distribution of their image gray levels [12]. The features can be used with a classifier to assign the class for the unknown object.

In this study, Gabor filter is used as an operator for extracting textural statistical properties. It has a sense of directionality and spatial frequency which are related to the basic texture properties. In Gabor filter based feature extraction, the FNAC input images are filtered with the filter bank and then a set of descriptors are computed from the resulting output images. Gabor filter's characteristics is a Gaussian signal, called as envelope, modulated by a cosine signal, called a carrier [13].

$$g_{\lambda,\theta,\varphi}(x,y) = e^{-\frac{(x'^2+\gamma^2 y'^2)}{2\sigma^2}} \cos\left(\frac{2\pi x'}{\lambda} + \varphi\right) \qquad (5)$$

where,

$$x' = x\cos\theta + y\sin\theta$$

$$y' = -x\sin\theta + y\sin\theta$$

The effective size of the Gaussian signal is determined by the standard deviation σ. The direction of the cosine function is determined by θ along with the phase offset ϕ. λ is the wavelength of the cosine function. An input image $f(x,y)$, $x,y \in X$ (X is the set of image points), is convolved with a two-dimensional Gabor function $g(x,y)$, $x,y \in$ X to obtain a Gabor feature image. The Gabor families of filters are generated for four frequencies 4, 8, 16 and 32 as well as four orientations 0, 45, 90 and 135 degrees. Each image in the training set and testing set are convolved with these filters. The statistical features mean, standard deviation, entropy, variance, energy, homogeneity, contrast and correlation are extracted and stored in feature library as listed in Table I.

TABLE I. Performance Analysis of Discrimination Models

Statistical Feature	Description
Mean	$\sum_{i,j} f(i,j)/N$
Standard Deviation	$\sum_{i,j} ((f(i,j)-\mu)^2/N)^{\frac{1}{2}}$
Entropy	$-\sum_{i,j} f(i,j) \log f(i,j)$
Variance	σ^2
Energy	$\sum_{i,j} f(i,j)^2$
Homogeneity	$\sum_{i,j} \frac{f(i,j)}{1+\lvert i-j \rvert}$
Contrast	$\sum_{i,j} f(i,j)\,(i-j)^2$
Correlation	$\sum_{i,j} f(i,j)\,(i-\mu_i)\,(j-\mu_j)/\sigma_i\sigma_j$

where, $f(i,j)$ is the gray level value for each pixel in the region of interest, N is the total number of pixels in the region of interest and μ_i, μ_j, σ_i, σ_j, σ_j^2 are means and standard deviations of $f(i,j)$.

IV. Neural Network Based Classification Models

Neural networks (NNs) are robust and flexible modeling techniques that attempt to imitate the basic structure and function of biological neurons to solve complex classification problems.

A. Elman Neural Network Classifier

The Elman Neural Network (ENN) is a simple recurrent neural network which consists of a two-layer back propagation network with an additional feedback connection from the output of the hidden layer to its input [14]. In a basic Elman network, in addition to the input unit, the hidden units and the output unit, there are also context units. The context units provide the network with a short term memory to maintain a copy of the previous values of its hidden layer. This means that interrelations between the current input and internal states are processed to produce the output, after training. Since the network can store information for future reference, it can learn temporal patterns as well as spatial patterns. A general architecture of Elman network is shown in Fig. 2.

The training objective of ENN is to recursively update the weights of each layer so that error is minimized. The Elman network has 'tansig' neurons in its hidden layer and 'purelin' neurons in its output layer. Each context node receives input from a single hidden node and sends its output to each node in the layer of its corresponding hidden node. Since the context nodes depend only on the activations of the hidden nodes from the previous input, the context nodes retain state information among inputs. The hidden layer with 'sigmoid' activation functions activates the output layer and refreshes the context layer with the current state of the hidden layer [15].

At a specific time *t*, the previous activations of the hidden units at time *t-1* and the current input, at time *t*, are used as inputs to the network. At this stage, the network acts as a feed forward network and propagates these inputs to produce the output.

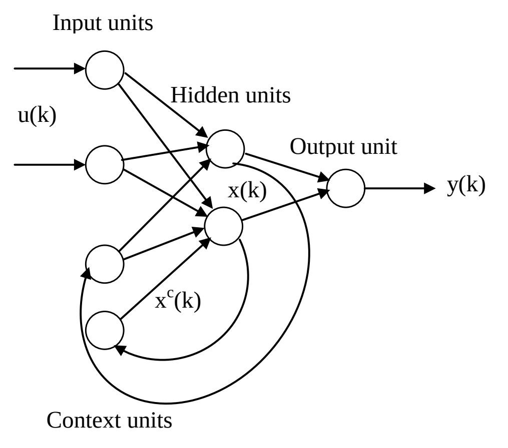

Fig. 2 Architecture of Elman neural network

The standard back propagation learning rule can be used to train the network. After this training step, the activations of the hidden units at time *t* are sent back through the recurrent links to the context units and saved there for the next training step at time *t+1*. During the beginning of the training process, the activations of the hidden units are unknown. Usually, they are set to one-half of their maximum range. For a sigmoidal activation function the initial values can be set to 0.5. For a hyperbolic tangent activation function they can be equated to 0.0.

The external input feature set derived by feature extraction methods to the network and output diagnostic result from the network are represented by $u(k)$ and $y(k)$ respectively. The total input to the i^{th} hidden unit is denoted as $v_i(k)$ and is given by,

$$v_i(k) = \sum_{j=1}^{n} w_{i,j}^{x}(k-1)x_j^c(k) + w_i^u(k-1)u(k) \qquad (6)$$

The output of the i^{th} hidden unit and j^{th} context unit are given by,

$$x_i(k) = f(v_i) \qquad (7)$$

$$X_j^c(k) = x_j(k-1) \qquad (8)$$

$$y(k) = \sum_{i=1}^{n} w_i^y(k-1)x_j(k) \qquad (9)$$

Where, $w_{i,j}^{x}(k-1), w_i^u$ and w_i^y are the weights of the links and *f* is a siginoidal activation function.

For the present work, Elman artificial neural network models are developed with a single hidden layer of 20 neurons and sigmoid activation functions for discriminating benign and malignant thyroid nodules. The feature sets derived from Gabor filter are used to train and test the ENN classifier. The statistical features mean, standard deviation, entropy, variance, energy, homogeneity, contrast and correlation are used as input variables to the network and diagnostic class is obtained from the network as the output.

B. Auto-associative Neural Network Classifier

An Auto-associative Neural Network (ANN) is a multi-layer perceptron network that maps identically the input pattern into output pattern. In the middle of the network, there is a layer that works as a bottleneck to perform reduction in the size of the data [16]. The basic architecture of an ANN is illustrated in Fig. 3. The input layer pattern is identified as, x_1, x_2, x_3,..., x_n. The weights are w_1, w_2, w_3 and w_4. The weights in the network are initially set to small random values. The error between the actual and expected output vectors is minimized. Then, the weights are modified with respect to input training patterns present in the input layer. Thus, the output vectors are produced by the ANN with continuous modifications in the weights and periodically compared with the input vectors.

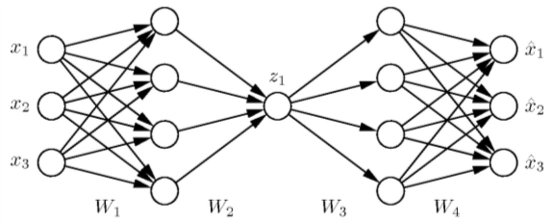

Fig. 3 Architecture of Auto-associative neural network

The learning process is stopped, when there is no difference between input and output vectors. During the testing phase, the ANN processes the input pattern and produces output pattern. The weights are adjusted to get input vectors as output vectors.

C. Results of the Discrimination Process

The discrimination process of thyroid FNAC can be performed under training phase and testing phase as shown in Fig. 4. In training phase, the statistical features are derived from segmented training set images of benign and malignant thyroid nodules and stored in the database. In the testing phase, the same set of statistical features are extracted from testing set images and are compared with the database using ENN and ANN classifiers. The training image set consists of 80 images (40 benign and 40 malignant images) whereas the testing image set has 30 images (10 benign and 20 malignant images).

The experiments on training and testing both the neural networks are conducted using MATLAB 2015a version and results are observed. A discrimination accuracy of 93.33% is obtained with sensitivity of 90% and specificity of 100% by ENN classifier when it uses the results of morphology segmentation and the features derived from Gabor filter with wavelength 4 and angle 45. However, ANN classifier reports a highest discrimination accuracy of 96.66% with sensitivity of 95% and specificity of 100% as given in Table II. The comparative analysis of all the discrimination models developed by the authors is summarized in Table III.

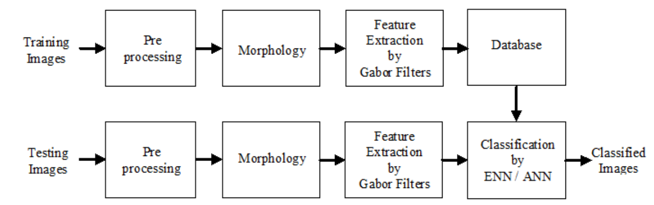

Fig. 4 Discrimination process

TABLE II. PERFORMANCE ANALYSIS OF DISCRIMINATION MODELS

Neural Network	Performance Analysis (%)		
	Discrimination accuracy	*Sensitivity*	*Specificity*
ENN	93.3	90	100
ANN	96.6	95	100

TABLE III. COMPARATIVE ANALYSIS OF DISCRIMINATION MODELS

Studies	Performance Analysis	
	Classifier	*Discrimination Accuracy (%)*
Gopinath et al. (7)	ENN	93.33
Gopinath et al. (8)	Multiple Classifier Fusion	96.66
Proposed discrimination system	ENN	93.33
	ANN	96.66

From Table III, it is evident that the discrimination model developed using auto-associative neural network outperforms and results around 3% increment in the discrimination accuracy compared with Elman neural network. Also, it is being a perfect competitive model for the discrimination model developed using multiple classifier fusion.

V. CONCLUSION

An automated pattern recognition system was developed to discriminate benign and malignant FNAC cytological images of thyroid nodules using Gabor filter features and ENN and ANN classifiers along with morphological segmentation technique. The discrimination results given by the classifiers were compared based on their accuracy, sensitivity and specificity. The ENN classifier reported a discrimination accuracy of 93.33% whereas the ANN classifier reported highest discrimination accuracy of 96.66% for the FNAC images segmented by morphology segmentation method for Gabor filter based features. These results conclude that ANN classifier performs better with a combination of mathematical morphology based image segmentation method and Gabor filter features.

REFERENCES

[1] S.A. Mahar, A. Husain, and N. Islam, "Fine needle aspiration cytology of thyroid nodule: Diagnostic accuracy and pitfalls," Journal of Ayub Medical College, vol. 18, pp. 26-29, 2006.

[2] P. Karakitsos, B. Cochand-Priollet, P.J. Guillausseau, and A. Pouliakis, "Potential of the back propagation neural network in the morphologic examination of thyroid lesions," Anal. Quant. Cytol. Histol., vol. 18, pp. 494-500, 1996.

[3] T. Wurflinger, J. Stockhausen, D. Meyer-Ebrecht, and A. Bocking, "Robust automatic coregistration, segmentation and classification of cell nuclei in multimodal cytopathological microscopic images," Comput. Med. Imaging Graph., vol. 28, pp. 87–98, 2003.

[4] O. Lezoray, and M. Lecluse, "Automatic segmentation and classification of cells from Bronchoalveolar lavage," Image Anal. Stereol., vol. 26, pp. 111–119, 2007.

[5] N.A. Shapiro, T.L. Poloz, V.A. Shkurupij, M.S. Tarkov, V.V. Poloz, and A.V. Demin, "Application of artificial neural network for classification of thyroid follicular tumors," Anal. Quant. Cytol. Histol., Vol. 29, pp. 87–94, 2007.

[6] X. Wang, S. Li, H. Liu, M. Wood, W.R. Chen, and B. Zheng, "Automated identification of analyzable metaphase chromosomes depicted on microscopic digital images," J. Biomed. Inform., vol. 41, pp. 264–271, 2008.

[7] A. Daskalakis, S. Kostopoulos, P. Spyridonos, D. Glotsos, P. Ravazoula, M. Kardari, I. Kalatzis, D. Cavouras, and G. Nikiforidis, "Design of a multi-classifier system for discriminating benign from malignant thyroid nodules using routinely H&E-stained cytological images," Comput. Biol. Med., vol. 38, pp. 196–203, 2008.

[8] B. Gopinath, and N. Shanthi, "Development of an Automated Medical Diagnosis System for Classifying Thyroid Tumor Cells using Multiple Classifier Fusion," Technology in Cancer Research and Treatment, vol. 14, pp. 653–662, 2015.

[9] B. Gopinath, and N. Shanthi, "Computer-aided diagnosis system for classifying benign and malignant thyroid nodules in multi-stained FNAB

cytological images," Australas. Phys. Eng. Sci. Med., vol. 36, pp. 219–230, 2013.

[10] http://www.papsociety.org/atlas.html

[11] N. Otsu, "A threshold selection method from gray-level histograms" IEEE Trans. Syst. Man Cybern., vol. 9, pp. 62–66, 1979.

[12] B. Julesz, E.N. Gilbert, L.A. Shepp, and H.L. Frisch, "Inability of humans to discriminate between visual textures that agree in second-order statistics revisited," Perception, vol. 2, pp. 391–405, 1973.

[13] N. Linder, J. Konsti, R. Turkki, E. Rahtu, M. Lundin, S. Nordling, C. Haglund, T. Ahonen, M. Pietikainen, and J. Lundin, "Identification of tumor epithelium and stroma in tissue microarrays using texture analysis," Diagn. Pathol., vol. 7, pp. 22, 2012.

[14] J.L. Elman, "Finding structure in time," Cogn. Sci. vol., 14, pp. 179–211, 1990.

[15] Q. Song, "On the weight convergence of Elman networks," IEEE Trans. Neural Netw., vol. 21, pp. 463–480, 2010.

[16] D. Hemmerling, "Voice pathology distinction using autoassociative neural networks," European Signal Processing Conference (EUSIPCO), 2017.